Transmission of the Oceanic Chlorophyll Fluorescence to the Top of the Atmosphere

Peter Schlüssel and Hartmut Graßl

UDC 551.463.5:535.37.1:551.593:547.979.7

Summary

Radiative transfer modelling for a coupled ocean-atmosphere system near 685 nm indicates a sufficiently high fluorescence signal of the chlorophyll a transmitted to the top of the atmosphere. However, only the shortwave half is seen at the top of the atmosphere, the longwave half is fully masked by atmospheric oxygen and water vapour absorption. The impact of atmospheric aerosol extinction on the signal transmission is almost negligible. The H_α line of the sun, atmospheric water vapour absorption, and chlorophyll absorption near 670 nm influence radiative transfer in the shortwave tail of the fluorescence line making the search for a baseline in order to eliminate the background radiation a difficult task.

Transmission der ozeanischen Chlorophyll-Fluoreszenz zum Außenrand der Atmosphäre (Zusammenfassung)

Die Strahlungsübertragungsgleichung wird für ein Atmosphäre-Ozean-System auf Grundlage der Matrix-Operator-Methode gelöst, um das Transmissionsverhalten der Atmosphäre in der Nähe der Chlorophyll-a-Fluoreszenz bei 685 nm im Hinblick auf die Fernerkundung des ozeanischen Phytoplanktons zu untersuchen. Während der kurzwellige Teil der Fluoreszenz vollständig zum Atmosphärenrand transmittiert wird, ist die langwellige Hälfte von der atmosphärischen Sauerstoff- und Wasserdampfabsorption völlig maskiert. Die Simulationsrechnungen zeigen, daß der Einfluß atmosphärischer Aerosole auf die Transmission des Signals nahezu vernachlässigbar ist. Dagegen stören eine H_α-Linie der Sonne, atmosphärische Wasserdampfabsorption und die Chlorophyllabsorption nahe 670 nm die Strahlungsübertragung des langwelligen Teils derart stark, daß die Suche nach einer Basislinie zur Eliminierung der Hintergrundstrahlung schwierig wird.

Transmission de la fluorescence chlorophylienne océanique vers la partie supérieure de l'atmosphère (Résumé)

L'équation de transmission du rayonnement pour un système combiné océan-atmosphère est résolue à l'aide de la méthode opérateur-matrice en vue de définir les caractéristiques de transmission de la fluorescence chlorophylienne-a à 685 nm en tenant compte de la reconnaissance à distance du phytoplancton océanique. Le spectre onde courte de la fluorescence est transmis entièrement à la partie supérieure de l'atmosphère alors que le spectre onde longue est entièrement masqué par l'absorption due à la vapeur d'eau et à l'oxygène dans l'atmosphère. Les calculs de simulation montrent que l'influence des aérosols sur la transmission du signal est quasiment négligeable. Par contre, la raie H_α du soleil, l'absorption par la vapeur d'eau atmosphérique et de la chlorophylle à environ 670 nm affectent la transmission du rayonnement si fortement qu'il est malaisé de rechercher une ligne de base en vue de supprimer le rayonnement ambiant.

1 Introduction

The quantitative determination of the phytoplankton concentration is not only desirable from the point of view of oceanic ecosystems, but also may affect climate via the assimilation of carbon dioxide. The unique and most efficient way to map phytoplankton is sounding from orbiting satellites. A measure of phytoplankton is the concentration of oceanic chlorophyll a.

The common technique of passive remote sensing of oceanic chlorophyll is to observe the "blue to green ratio" of reflected solar radiation. At present, this method is applied to data from Coastal Zone Colour Scanner (CZCS) on board NIMBUS-7 spacecraft by different groups (Dörffer [1981]; Gordon, Clark and Hovis [1980]; Morel [1980]; Quenzel and Kästner [1978]). Normally, they compare upwelling radiances at 443 and 550 nm and thus hope to estimate chlorophyll content; because, for example, greener water indicates a higher chlorophyll concentration. A central disadvantage of this method is the change of the "blue to green ratio" by the atmosphere which can be calculated for an atmosphere with molecular scattering only, but varies in a wide range with atmospheric turbidity.

Another possible method to map chlorophyll from space is to measure its fluorescence near 685 nm. The fluorescence line has a halfwidth of about 12.5 nm (half width at half maximum) and thus its remote sensing with contemporary radiometers is possible as shown by Neville and Gower [1977]. A demonstration of the remote mapping of the chlorophyll fluorescence has already been given by Gower and Borstad [1981] who measured a good transmission of the oceanic chlorophyll fluorescence through the lower atmosphere in an airborne experiment.

In order to investigate the feasibility of measuring chlorophyll fluorescence from space, we have solved the radiative transfer equation by the matrix-operator method for a coupled ocean-atmosphere system. We account for scattering by air molecules, absorption by water vapour and oxygen molecules, extinction by atmospheric aerosol particles, water molecules, phytoplankton, sediments and "Gelbstoff". Thereby, a main point is the absorption of molecular oxygen and water vapour in the vibration rotation bands near the chlorophyll fluorescence.

2 Basic equations

The spectral radiance I_ν received at satellite altitude H from direction $\boldsymbol{s}$ due to backscattering of solar radiation by the ocean-atmosphere system (flat ocean) is described by the radiative transfer equation (Goody [1964]), presented in the formally integrated form

$$I_\nu(H, \boldsymbol{s}) = I_\nu(H_0, \boldsymbol{s}^*) \exp(-\tau_\nu) + \int_0^{\tau_\nu} J_\nu(H', \boldsymbol{s}) \exp(-\tau_\nu(H, H'))\, \mathrm{d}\tau_\nu \qquad (1)$$

with τ_ν total spectral optical depth of the ocean-atmosphere system
$\tau_\nu(H, H')$ spectral optical depth between satellite height H and layer height H'
H_0 ocean bottom
$\boldsymbol{s}^*$ direction within the ocean, accounting for refraction at the surface
$J_\nu(H', \boldsymbol{s})$ source function at H' into direction $\boldsymbol{s}$

Relevant sources in the spectral domain of solar radiation result from multiple scattering by molecules and particles and – in our special case – also from chlorophyll a fluorescence at 685 nm.

The source function J_ν^s for scattering integrates radiances from all solid angles $d\omega'$ scattered into direction s

$$J_\nu^s(H, s) = \frac{\omega_{0\nu}}{4\pi} \int_0^{4\pi} P_\nu(s_0, s)\, I_\nu(H, s_0)\, d\omega' \tag{2}$$

The single scattering albedo $\omega_{0\nu} = s_\nu / e_\nu$ compares the scattering coefficient s_ν to the extinction coefficient e_ν. The phase function $P_\nu(s_0, s)$ specifies the energy scattered from direction s_0 into s.

The interaction between radiation and fluorescent matter in a volume element ΔV relative to the total incident irradiance $\int_{\Delta\nu_E} h_{\nu_E'}(H)\, d\nu_E'$ is defined by the volume fluorescence function (Gordon [1979]):

$$\beta_{\nu_F, \nu_E}(s_0, s) = \frac{L_{\nu_F}(H, s)}{\Delta V \int_{\Delta\nu_E} h_{\nu'_E}(H)\, d\nu'_E} \qquad \text{given in } m^{-1}/(sr \cdot cm^{-1}) \tag{3}$$

where $L_{\nu_F}(H, s)$ denotes the fluorescent emittance in $W \cdot sr^{-1} \cdot cm^{-1}$ at wavenumber ν_F at height H into direction s excited by photons at larger wavenumbers ν_E entering ΔV at H from s_0. Thus, the source term due to fluorescence becomes

$$J_\nu^F(H, s) = \int_{\nu_{E_1}}^{\nu_{E_2}} \int_0^{4\pi} \beta_{\nu_F, \nu'_E}(s_0, s)\, I_{\nu'_E}(H, s_0)\, d\omega\, d\nu'_E \tag{4}$$

To complete the definition of the volume fluorescence, the coefficient of the fluorescence

$$\Phi_{\nu_F, \nu_E} = \int_0^{4\pi} \beta_{\nu_F, \nu_E}\, d\omega \qquad \text{given in } m^{-1} \cdot cm^{-1} \tag{5}$$

must be related to the quantum efficiency η_{ν_F, ν_E}, the ratio of the emission rate of photons from ΔV at wavenumbers between ν_F and $\nu_F + \Delta\nu_F$ to the absorption rate in ΔV for photons with wavenumbers between ν_E and $\nu_E + \Delta\nu_E$:

$$\eta_{\nu_F, \nu_E} = \frac{\nu_F}{\nu_E} \frac{\Phi_{\nu_F, \nu_E}\, \Delta\nu_F}{a_{\nu_E}} \tag{6}$$

with a_{ν_E} absorption coefficient of the fluorescent matter in ΔV.

3 Radiative transfer model

A radiative transfer model applied to a coupled ocean-atmosphere system in the solar spectral domain must be able to handle occurring large optical depths as well as multiple scattering in ocean and atmosphere. An appropriate model has been developed by Fischer [1984] on the basis of the matrix-operator method, which has been summarized by Plass, Kattawar, Catchings [1973]. The model discretizes optical depth and solid angle. The optically active medium is assumed to be horizontally homogeneous, i.e. plane parallel. The atmosphere is divided into five, the shallow ocean (depth: 30 m) into two layers only, a fictive intermediate layer simulates refraction and reflection at the sea surface.

The approximation flat surface has been shown to be justified for many remote sensing conditions by Fischer and Graßl [1984]. The restriction to shallow ocean does not hamper the discussion of most cases, since an extinction coefficient of only 0.2 m^{-1} frequently occurring in ocean waters already makes the bottom contribution negligible. The azimuthal dependence of the radiative transfer is eliminated by averaging, consequently the angular distribution of radiances is limited to a fixed number of zenith angles ($N = 6$). Keeping in mind that a simple Gaussian quadrature does not allow to simulate nadir observation of the backscattering by suspended matter, we have applied the socalled Lobatto integration. Despite azimuthal averaging, the Lobatto integration allows the exact computation of upwelling radiances in nadir direction (Fischer [1984]), the main viewing direction of orbiting radiometers and air planes. A slight disadvantage of this dicretization, is the fixation of solar zenith angles to be used for a given number of angular intervals. Here, with 6 intervals including the nadir direction, solar zenith angles between 19 and 82 degrees are simulated. Further zenith angles must be included for scattered radiation in the ocean accounting for the accumulation of all the "atmospheric" zenith angles in a cone between nadir and the angle of total reflection (Table 1).

At the sea surface the radiation is refracted following Snellius' law. Assuming a flat surface, valid for calculation of radiances near nadir direction (Austin [1974]; Fischer [1984]), we compute the reflection at the sea surface by Fresnel's formula. White caps and surface bubbles are neglected, because they are not important at rather low wind speeds, a prerequisite for remote ocean colours sensing.

The bottom of the ocean has been approximated by a Lambert reflector with an albedo of 1 percent. This approximation is certainly not too coarse, because the turbid ocean attenuates radiation to almost negligible values at the bottom.

Scattering by air and water molecules according to Rayleigh's theory is applied, as well as the particle scattering described by Mie's theory for atmospheric aerosol particles, phytoplankton, and sediments. The corresponding phase functions are shown in Fig. 1.

Table 2 displays a summary of the optical parameters for margins and centre of the spectral interval considered.

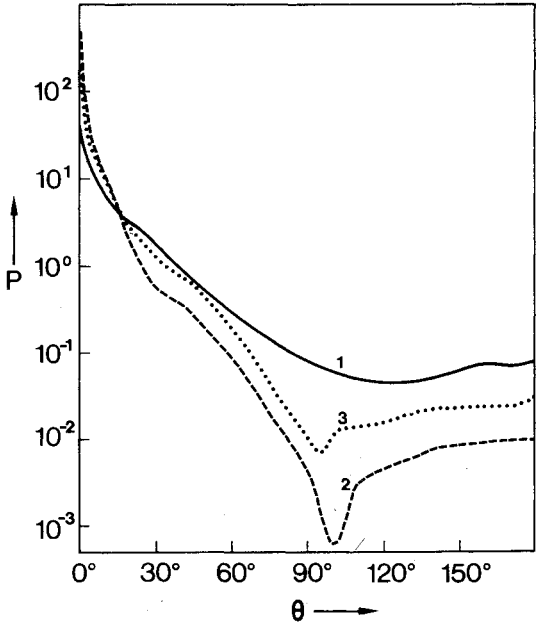

Fig. 1. Phase functions for atmospheric aerosol (1), phytoplankton (2), and sediments (3) (Fischer [1984])

The fluorescence-exciting radiation field in the ocean must be calculated in order to obtain the volume fluorescence function. This is done for 5 wavelengths between 390 and 685 nm representing the entire spectral domain, thus assuming that radiation outside this range does not excite chlorophyll fluorescence. Fluorescence is considered to be isotropic.

Table 1

Zenith angles in the atmosphere and ocean used in radiative transfer calculations

atmosphere	ocean
0.00°	0.00°
19.11°	14.21°
34.99°	25.46°
50.74°	36.48°
66.45°	43.41°
82.15°	47.95°
	60.37°
	80.52°

Table 2

Optical parameters

wavelength:	nm	654	685	712
solar irradiance: (Labs and Neckel [1970])	$W/m^2\,\mu m$	157.5	148.9	139.7
ozone absorption: (Dütsch [1970])	1/atm*cm	$5.5 \cdot 10^{-2}$	$3.0 \cdot 10^{-2}$	$1.9 \cdot 10^{-2}$
atmospheric aerosol: Hänel Model HMF7 (Fischer [1984])				
extinction $e/e_{865\,nm}$		1.01	1.0	0.98
single scattering albedo		0.85	0.85	0.85
chlorophyll: (Yentsch [1960]; Prieur and Sathyendranath [1981])				
absorption	1/m	$4.19 \cdot 10^{-2}$	$4.86 \cdot 10^{-2}$	$3.64 \cdot 10^{-2}$
scattering	1/m	$1.35 \cdot 10^{-1}$	$1.21 \cdot 10^{-1}$	$1.26 \cdot 10^{-1}$
single scattering albedo		0.736	0.714	0.778
sediments: (Prieur and Sathyendranath [1981])				
absorption	1/m	$3.19 \cdot 10^{-2}$	$3.06 \cdot 10^{-2}$	$2.95 \cdot 10^{-2}$
scattering	1/m	$1.45 \cdot 10^{-1}$	$1.39 \cdot 10^{-1}$	$1.33 \cdot 10^{-1}$
single scattering albedo		0.82	0.82	0.82
"Gelbstoff" absorption: (Højerslev [1979])	1/m	$1.22 \cdot 10^{-4}$	$7.9 \cdot 10^{-3}$	$5.41 \cdot 10^{-3}$
pure water absorption: (Morel [1974])	1/m	0.38	0.48	1.1
fluorescence quantum efficiency: (Kiefer [1973])			2%	

* 1 atm = 1013.25 hPa

4 Absorption by molecular oxygen and water vapour

The absorption by molecular oxygen and water vapour in the vibration rotation bands near the chlorophyll fluorescence is explored by means of Lorentz's theory of collision broadening. The contribution by resonance broadening is small for weak absorption bands such as those encountered. Doppler line widths are also small compared to Lorentz line widths for gases in the lower atmosphere below about 40 km (Rodgers and Walshaw [1966]). For a refined treatment, H_2O lines might be slightly modified if Voigt line shapes are introduced. For wave numbers $>10^3$ the absorption coefficient at wavenumber ν in a certain distance from an absorption line at ν_0 is characterized by its line intensity S and the halfwidth α:

$$k_\nu = \frac{S}{\pi} \frac{\alpha}{(\nu - \nu_0)^2 + \alpha^2} \tag{7}$$

S mainly depends upon line strength S_0, temperature T, and on number density n of the absorbing molecule

$$S = S_0 n \left(\frac{T_0}{T}\right)^\delta \exp\left(-\frac{E_0}{k_0}\left(\frac{1}{T} - \frac{1}{T_0}\right)\right) \tag{8}$$

with k_0 Boltzmann's constant

δ molecular constant depending upon degrees of freedom for rotation ($\delta = 1$ for linear molecules such as O_2, $\delta = 1.5$ for nonlinear molecules such as H_2O)

E_0 lower state energy

The halfwidth reads

$$\alpha = \alpha_0 \frac{p}{p_0} \left(\frac{T_0}{T}\right)^{1/2} \tag{9}$$

where α_0 halfwidth at p_0, T_0

p pressure

p_0 = 1013.25 hPa (= 1 atm)

T_0 = 296 K

The high resolution (0.05 cm^{-1}) absorption spectra computed with a line-by-line code from the aforementioned line parameters, using a compilation by McClatchey and Rothman [1978], are compared (see Fig. 2 as an example) to measured high resolution sun spectra (Delbouille, Roland and Neven [1981]). The sun spectrum is measured at a height of 3.58 km, and so its lines – due to the reduced absorber amount – are comparably weak. A curiosity is the unexplained spectral shift of one spectrum against the other by 0.19 nm. A disturbance at the shortwave tail of the chlorophyll fluorescence is the strong H_α line of the sun. Its absorption reduces the solar irradiance at 656.3 nm to 15 % of the nearby values. The halfwidth of the line is almost 0.07 nm (Fig. 3). Before inserting the absorption spectra into the radiative transfer model simulating radiometer signals they have to be averaged over the appropriate spectral interval of the radiometer. 20 wavenumbers corresponding to ≈ 1 nm at these frequencies around the fluorescence line are chosen here with reference to present technological expectations. Again, the comparison to the measured spectrum shows only a coarse conformity (Fig. 4).

The transmission functions, after averaging, are fitted with exponential sums for use in the radiative transfer model.

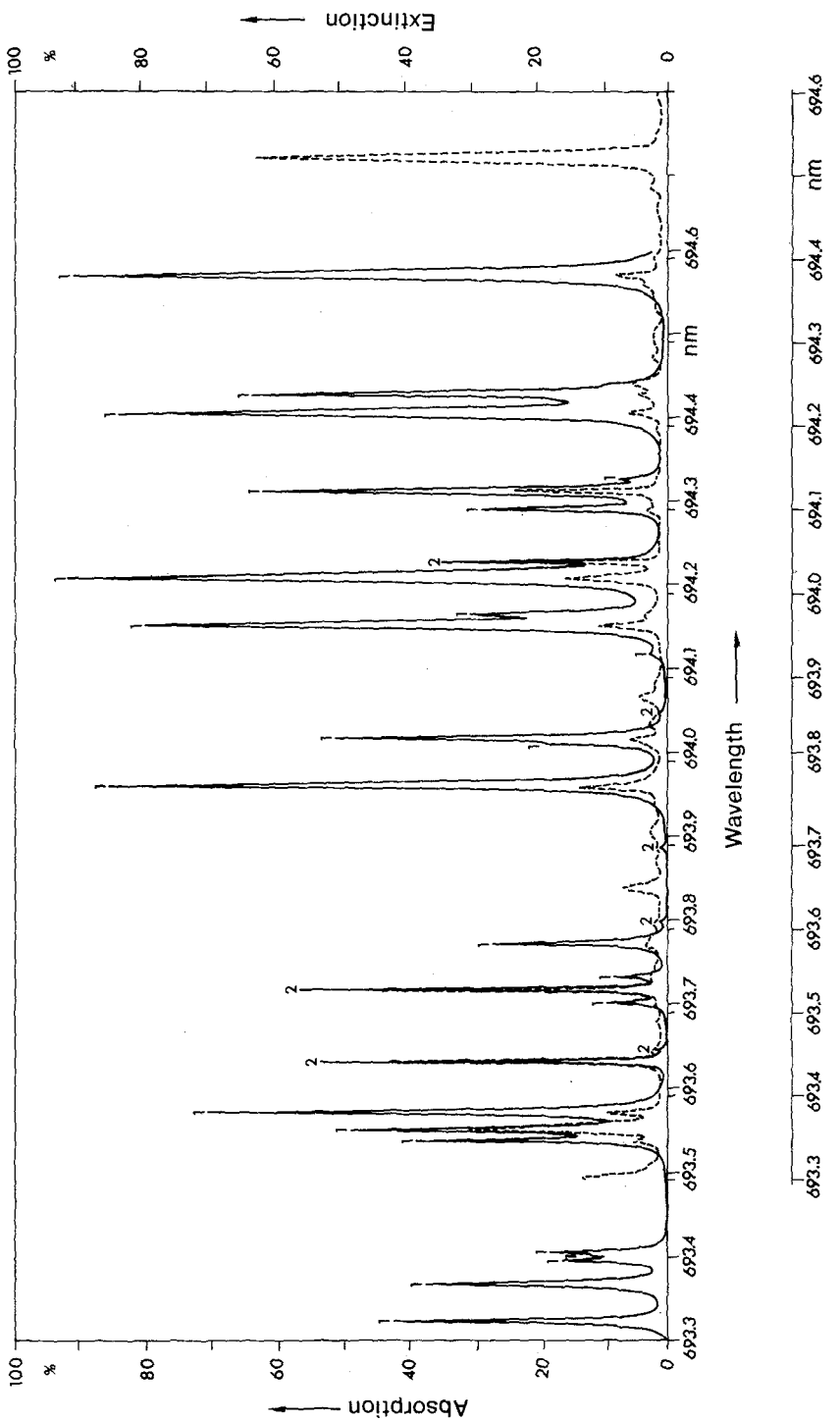

Fig. 2. Computed absorption spectrum (from McClatchey and Rothman, absorption line parameters compilation [1978]) for a standard atmosphere with 2.34 g/cm^2 H_2O; 1 = H_2O lines, 2 = O_2 lines (continuous plot, upper abscissa, left ordinate) in comparison to the measured solar spectrum attenuated by the upper atmosphere (Delbouille, Roland and Neven [1981] – dashed in line, lower abscissa, right ordinate)

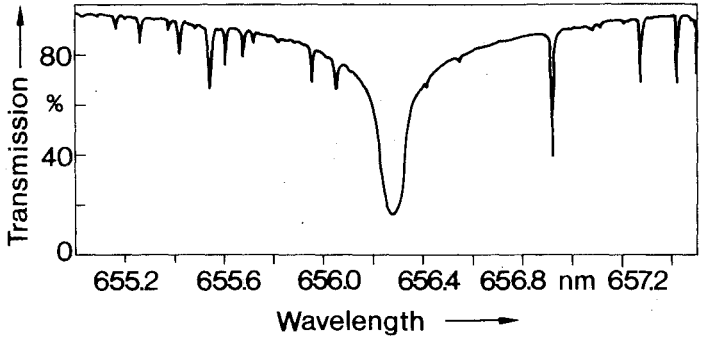

Fig. 3. H_α-line in the measured sun spectrum from Delbouille, Roland and Neven [1981]

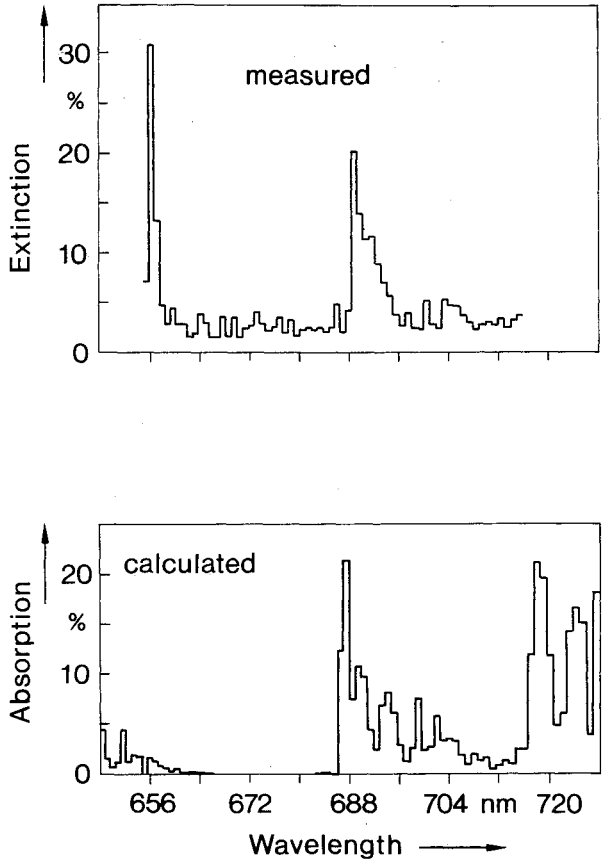

Fig. 4. Above: Averaged (20 cm^{-1}) extinction spectrum from Delbouille, Roland and Neven [1981]
Below: Averaged (20 cm^{-1}) absorption spectrum, calculated from absorption line parameters (McClatchey and Rothman [1978]); 2.34 g/cm^2 H_2O content; line wings at a distance > 2/cm from their line centre are neglected

5 Model results

The transmission of the chlorophyll fluorescence to the top of the atmosphere is calculated for 61 spectral intervals approximately 1 nm wide (exact width: 20 cm^{-1}) in the 655 to 711 nm domain.

The upward radiances for 5 solar zenith angles between 19 and 82 degrees at the ocean surface and at the top of the atmosphere clearly show the masking of radiance leaving the ocean by the atmosphere (Fig. 5).

The variation of the radiances at the top of the atmosphere, due to variable quantities of suspended oceanic material, is very weak in the spectral region considered. The influence of "Gelbstoff" absorption on the radiation field is negligible. Backscattering of solar radiation, due to chlorophyll and sediments, causes only a weak increase in the upwelling radiances at the top of the atmosphere (Fig. 6). These small variations indicate that a

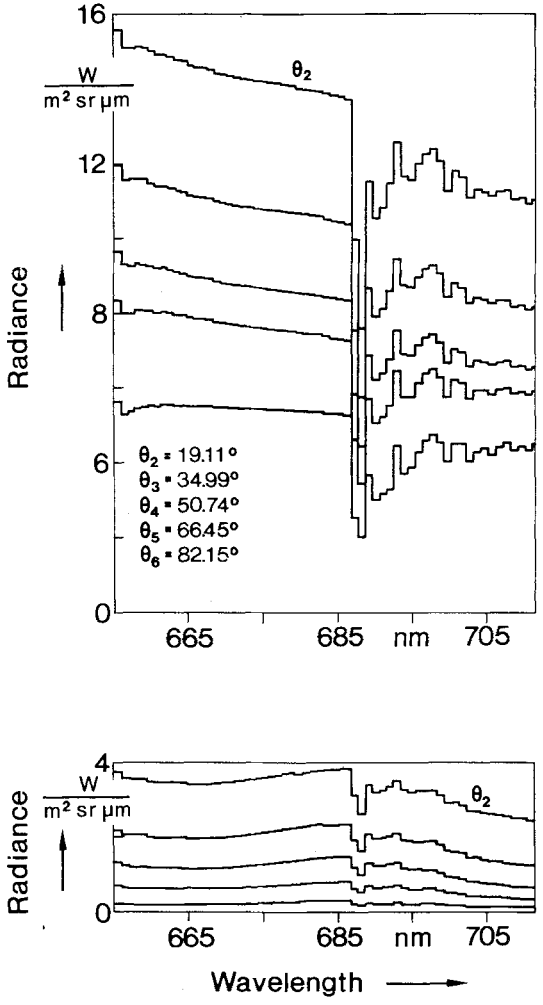

Fig. 5. Upward radiances for 5 solar zenith angles Θ at sea surface (below) and at the top of the atmosphere (above)

separation of different oceanic suspensions – for the spectral domain adopted – is impossible from elastic backscattering only. This fact will be confirmed if variations of atmospheric constituents, such as water vapour and aerosol particles, are included (Fig. 7). A doubling of the amount of water vapour reduces upwelling radiances up to a factor of 8 (strongly depending upon spectral position) if compared to a 3 mg/m^3 change in chlorophyll. Halving the number of aerosol particles may increase the spectral signal up to 13 times. The chlorophyll fluorescence increases the upwelling radiances three times in comparison to elastic backscattering by chlorophyll.

The effect of the spectrally broad "Gelbstoff" fluorescence near 500 nm on the radiation field has not been modelled. Its great variability in strength and shape is still not understood and needs further investigations. However, this feature may slightly increase the upwelling radiances near 685 nm.

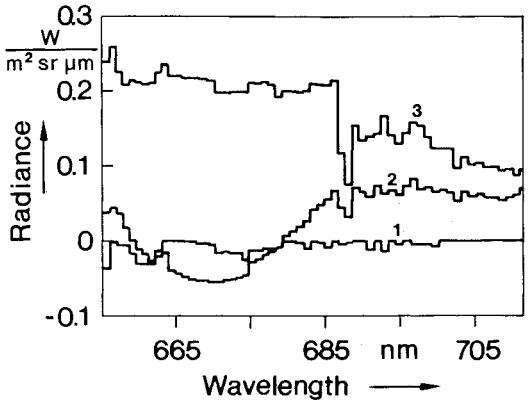

Fig. 6. Variation of upwelling radiances at the top of the atmosphere for a zenith angle $\Theta_4 = 50.74°$ of the sun caused by 1 mg/l "Gelbstoff" (1), 3 mg/m^3 phytoplankton (2) or sediments (3)

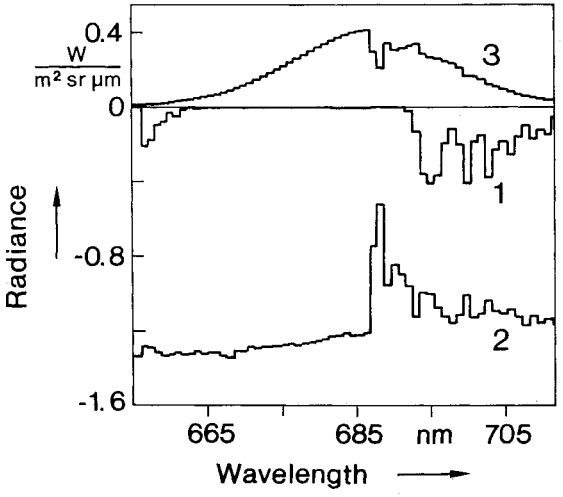

Fig. 7. Variation of upwelling radiances at the top of the atmosphere (sun's zenith angle $\Theta_4 = 50.74°$) for a doubling of atmospheric water vapour content (1), halving the aerosol content (2) or including the fluorescence into a turbid ocean (3)

6 The separation of the fluorescence signal from the background radiation

The oceanic reflection spectrum of solar radiation shows a maximum in the region near 550 nm, and a strong decrease to 700 nm. Fitting a baseline through this background spectrum, fixed at two wavelengths on both sides of the fluorescence line, equivalent to two window channels, enables the measurement of the height of the fluorescence peak above this baseline (Neville and Gower [1977]). The wavelengths have to be chosen very carefully, preferably near 650 and 715 nm, in order to avoid disturbances by variation in the H_2O absorption bands. The regions with least absorption are at 655.3 and 711.2 nm which are chosen here to fix the baseline, despite the disturbance by the solar line at 656 nm (Fig. 8).

The relative radiance spectra at the sea surface and above the atmosphere, determined with the linear baseline approach, show a good transmission of the shortwave half of the fluorescence line while the longwave half is fully masked by oxygen and water vapour absorption. However, the height of the signal outside the atmosphere – despite a rather low extinction in the atmosphere – is generally smaller than the peak at sea surface. This reduction is caused by the parabolic shape of the background spectrum at the top of the atmosphere, in contrast to the linear baseline chosen. Another distortion of the linear approach is caused by the chlorophyll absorption line near 670 nm that draws down the shortwave tail of the fluorescence signal beneath the baseline. A parabolic baseline fitted at three points outside the fluorescence line (suggested by Neville and Gower [1977]) or measuring of the difference of radiances at 670 and 685 nm would be a superior approach.

In practice, the aforementioned choice of the shortwave reference point must be rejected, because of the solar line that reduces the solar radiation field at 656 nm. The present simulation neglects this fact. A small shift in wavelength, however, can avoid this disturbance.

The impact of variable atmospheric water vapour and aerosol content upon the fluorescence detection from space is small (Fig. 9). A doubled water vapour content increases the fluorescence peak centre by 9.9%, due to stronger absorption at the longwave reference of the baseline. Almost the same effect is caused by a halved aerosol content. The peak height increases by 8.6%. A variation of the fluorescence efficiency (equivalent to a variation in chlorophyll content) demonstrates the substance specific reaction of the signal at the top of the atmosphere.

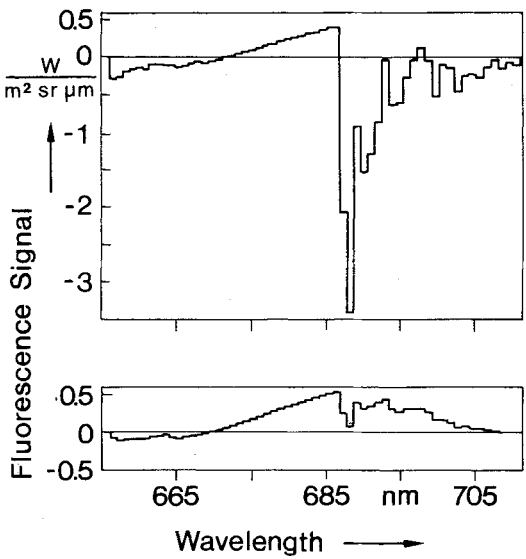

Fig. 8. Fluorescence signal extracted by the linear baseline approach at sea surface (below) and at the top of the atmosphere (above) ($\Theta_4 = 50.47°$)

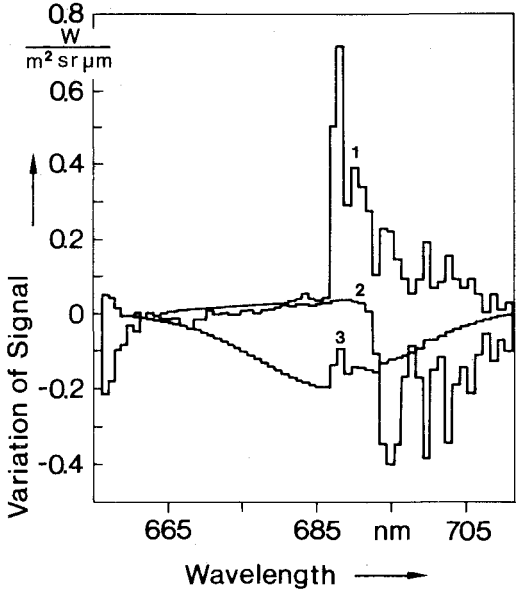

Fig. 9. Variation of the fluorescence signal at the top of the atmosphere caused by halving the atmospheric aerosol content (1), doubling the atmospheric water vapour content (2) or halving the fluorescence efficiency (3) ($\Theta_4 = 50.47°$)

7 Conclusions

The shortwave half of chlorophyll fluorescence at 685 nm is transmitted to the top of the atmosphere, thus enabling the detection of oceanic chlorophyll from space. The longwave half of the fluorescence line is fully masked by atmospheric oxygen and water vapour absorption, while the shortwave half is almost undisturbed by the atmosphere. The atmospheric aerosol extinction has nearly no influence upon the remote sensing of chlorophyll via its fluorescence if two nearby window channels are adopted for the definition of a background baseline. A main point that needs further consideration, is a search for the most efficient separation of the fluorescence signal from background radiation. If a baseline approach is applied, the reference channels must be chosen very carefully in order to avoid the impacts of solar lines and the water vapour absorption. Our suggestion is to measure the difference of radiances between peak chlorophyll absorption at 670 nm and peak fluorescence at 685 nm as a quantity for chlorophyll thus using two specific spectral features of chlorophyll at the same time.

Acknowledgement

The authors express their gratitude to Dr. J. Fischer for helpful discussions and the permission to use his computer programme for simulating the radiative transfer in a coupled ocean-atmosphere system.

References

Austin, R. W., 1974: The remote sensing of spectral radiance from below the ocean surface. In: Optical aspects of oceanography. (Ed.: N. G. Jerlov and E. Steemann Nielsen.) New York: Academic Pr. pp. 317–344.

Delbouille, L., G. Roland and L. Neven, 1981: Photometric atlas of the solar spectrum from λ 3000 to λ 10 000. Liège: Institut d'Astrophysique de l'Université, Observatoire Royal de Belgique. [Data tape.]

Dörffer, R., 1981: Factor analysis in the ocean colour interpretation. In: Oceanography from space. Proc. of the COSPAR (Committee for Space Research)/SCOR (Scient. Committee for Oceanic Research)/IUCRM (Inter-Union Commiss. Radio Meteorol.) Symposium held 1980 in Venice. New York: Plenum Pr. pp. 339–345.

Dütsch, H. U., 1970: Absorptionskoeffizienten des Ozons. In: Meteorologisches Taschenbuch. Bd. 2. (Ed.: F. Linke und F. Bauer.) p. 255.

Fischer, J., 1984: Fernerkundung von Schwebstoffen im Ozean. Hamburger Geophys. Einzelschr. (A) 65.

Fischer, J. and H. Graßl, 1984: Radiative transfer in an atmosphere-ocean-system: An azimuthally dependent matrix-operator approach. Appl. Optics. **23**, April issue.

Goody, R. M., 1964: Atmospheric radiation. P. 1. Oxford: Claredon Pr. XI, 436 pp.

Gordon, H. R., 1979: Diffuse reflection of the ocean, the theory of its augmentation by chlorophyll a fluorescence at 685 nm. Appl. Optics. **18**, 1161–1166.

Gordon, H. R., D. K. Clark and W. A. Hovis, 1980: Phytoplankton pigments from the NIMBUS-7 Coastal Zone Colour Scanner: Comparison with surface measurements. Science. **210**, 63–66.

Gower, J. F. R. and G. Borstad, 1981: Use of the in vivo fluorescence line at 685 nm for remote sensing surveys of surface chlorophyll a. In: Oceanography from space. Proc. of the COSPAR (Committee for Space Research)/SCOR (Scient. Committee for Oceanic Research)/IUCRM (Inter-Union Commiss. Radio Meteorol.) Symposium held 1980 in Venice. New York: Plenum Pr.

Højerslev, N. K., 1979: On the origin of yellow substances in the marine environment. Proc. Workshop on the Eurosep OCS Experiment, Oct. 1979.

Kiefer, D. A., 1973: Fluorescence properties of natural phytoplankton populations. Mar. Biol. **22**, 263–269.

Labs, D. and H. Neckel, 1970: Transformation of the absolute solar radiation data into the "International practical temperature scale of 1968". Solar Phys. **15**, 79–87.

McClatchey, R. A. and L. S. Rothman, 1978: Atmospheric absorption line parameters compilation. Bedford, Mass.: Air Force Geophysics Laboratories. [Data tape.]

Morel, A., 1974: Optical properties of pure water and pure sea water. In: Optical aspects of oceanography. (Ed.: N. G. Jerlov and E. Steemann Nielsen.) New York: Academic Pr. pp. 1–24.

Morel, A., 1980: In-water and remote measurements of ocean color. Bound. Layer Meteorol. **18**, 177–201.

Neville, R. A., and J. F. R. Gower, 1977: Passive remote sensing of phytoplankton via chlorophyll a fluorescence. J. Geophys. Res. **82**, 3487–3493.

Plass, G. N., G. E. Kattawar and G. E. Catchings, 1973: Matrix-operator theory of radiative transfer. Appl. Optics. **12**, 314–329.

Prieur, L. and S. Sathyendranath, 1981: An optical classification of coastal oceanic waters based on the specific spectral absorption curves of phytoplankton pigments, dissolved organic matter and other particulate materials. Limnol. Oceanogr. **26**, 671–689.

Quenzel, H. and M. Kästner, 1978: Remote sensing of chlorophyll in the ocean: Masking effects of the atmosphere. Wiss. Mitt. Univ. München. Nr. 33.

Rodgers, C. D. and C. D. Walshaw, 1966: The computation of infra-red cooling rate in planetary atmospheres. Quart. J. Roy. Met. Soc. **92**, 67–92.

Yentsch, C. S., 1960: The influence of phytoplankton pigments on the colour of seawater. Deep-Sea Res. **7**, 1–9.

Eingegangen am 22. März 1984

Angenommen am 26. Juni 1984

Anschrift der Verfasser:
Dipl.-Met. Peter Schlüssel, Prof. Dr. Hartmut Graßl
Institut für Meereskunde an der Universität Kiel, Düsternbrooker Weg 20, 2300 Kiel 1